Microchimica Acta, Volume 187, Issue 12, December 2020, Article number 663
DOI:10.1007/s00604-020-04603-1

Long-Period Grating Fiber-Optic Sensors Exploiting Molecularly Imprinted TiO_2 Nanothin Films with Photocatalytic Self-Cleaning Ability

Tao Wang[1], Sergiy Korposh[2], Stephen James[3], and Seung-Woo Lee[1]*

[1]*Graduate School of Environmental Engineering, The University of Kitakyushu, 1-1 Hibikino, Kitakyushu 808-0135, Japan*

[2]*Optics and Photonics Group, Department of Electrical and Electronic Engineering, University of Nottingham, Nottingham, NG7 2RD, UK*

[3]*Engineering Photonics, School of Aerospace, Transport and Manufacturing, Cranfield University, Cranfield, Bedford MK43 0AL, UK*

* Corresponding author. Tel.: +81-93-695-3293; fax: +81-93-695-3384; e-mail: leesw@kitakyu-u.ac.jp

Abstract

Highly sensitive and selective long period grating (LPG) fiber-optic sensors modified with molecularly imprinted TiO_2 nanothin films were fabricated. The films were deposited onto the surface of the optical fiber via liquid phase deposition (LPD), using tetrakis(*N*-methylpyridinium-4-yl)porphyrin (TMPyP) as a template. Three LPG resonance bands were monitored during film deposition, which was of duration 4.5 h. Prior to template removal, heat treatment at 60 °C under high-humidity conditions led to an increase in refractive index of the TiO_2 film, evidenced by changes in the central wavelengths of the attenuation bands. After template removal using HCl solution (0.01 M), the TMPyP-imprinted film-modified LPG sensor showed higher sensitivity to the template molecule than to the structurally-related guest molecules. This was measured at the 1st and 2nd resonance bands, with wavelengths ranging from 690 nm to 738 nm and 815 nm to 905 nm, respectively. No selective binding of the template was observed with a non-imprinted TiO_2 film prepared in the same manner. Furthermore, the heat-treated imprinted films exhibited a substantial enhancement of photocatalytic activity for template irradiation. In particular, the self-cleaning property of the imprinted film-modified LPG sensor under ultraviolet irradiation led to highly efficient and selective

binding to the template. The mechanism of the interaction between the template and the TiO_2 matrix was investigated by UV–vis and Fourier-transform infrared (FTIR) spectroscopies. Additionally, morphological studies using scanning electron microscopy (SEM) were conducted.

Keywords: Long-period grating (LPG), molecular imprinting, liquid phase deposition (LPD), TiO_2 nanothin film, photocatalyst

1. Introduction

Recent applications of imprinted nanomaterials in bio and chemical sensors have received tremendous attention from the viewpoints of materials chemistry and surface chemistry because the molecular imprinting technique is considered to be an alternative tool for artificially realizing the molecular recognition in the biological system [1–5]. In particular, molecularly imprinted thin films have many advantages, including a quick response time and high sensitivity and selectivity [6]. Different methodologies have been employed for the preparation of molecularly imprinted films, such as organically modified sol–gel methods [7], the layer-by-layer (LbL) technique [8], liquid phase deposition (LPD) [9], and spin coating [10]. Silica gel [11] and organic polymers [12] can also be used for the fabrication of molecularly imprinted films, in which templates can be embedded via cross-linking of matrix monomers. We reported previously that the surface sol–gel process can facilitate the molecular imprinting of several organic substances in titanium oxide (TiO_2)-based organic-inorganic hybrid thin films, which can be formed on several devices to create sensors [13–16]. There are several advantages when using TiO_2 as a matrix for molecular imprinting, including its high affinity to organic and biological molecules, compatibility with complex components, and non-toxicity. In particular, the photocatalytic properties of TiO_2 can allow the molecular imprinting technique to be

explored for practical applications, for instance, photocatalytic degradation and selective removal of pesticides or herbicides [17], drugs [18,19], and other toxic chemicals [20,21] released in nature.

LPD is a well-known method for the preparation of metal oxide films from aqueous solutions [22,23]. Compared to other deposition techniques, the LPD technique is a low-temperature, low-cost, and reliable method and it offers lower equipment costs (as it is based on aqueous precursors), is energy efficient and highly flexible. The density of thin films prepared by LPD is higher than that of films prepared by other methods, such as vapor deposition and sol–gel methods. Thus, LPD may be well suited to imprinting biological compounds. TiO_2/organic hybrid thin films prepared via LPD have been used for the recognition of proteins [22] and *L*-glutamic acid [23]. Furthermore, TiO_2 has been shown to be an excellent photocatalytic material [24,25] and its nanoscale films have been investigated for applications in areas such as photodepollution [26], self-cleaning [27], and super-hydrophilic coating [28].

An optical fiber long-period grating (LPG) is produced by the periodic modulation of the refractive index (RI) of the core of the optical fiber and results in the coupling of light between the core mode and the cladding modes [29]. The characteristics of the coupling between the modes is dependent on the RI of the medium surrounding the LPG. The combination of an LPG and nanomaterials may allow the fabrication of highly sensitive sensors that could specifically bind target chemical species [30]. We have previously reported optical fiber LPG sensors based on a mesoporous film composed of alternate layers of silica (SiO_2) nanoparticles and polymers for the detection of organic compounds [31] and ammonia [32]. Molecular imprinting-based fiber-optic sensors have been intensively developed for non-labeled detection of complex biomolecules [33,34].

In this study, we examined molecularly imprinted TiO_2 nanothin films using tetrakis(*N*-methylpyridinium-4-yl)porphine (TMPyP) as a template, which were deposited onto optical fiber LPGs operating at the phase-matching turning point with the aim of developing novel, highly sensitive optical fiber sensors. This is the first report of the application of molecular imprinting based on TiO_2 nanothin films to optical fiber sensors. The TMPyP/TiO_2 hybrid film was fabricated via LPD, which provides a uniform film structure. The selectivity of the LPG sensor was tested using aromatic organic acid compounds. The mechanism of the interaction between the template and the TiO_2 matrix was investigated by UV–vis and Fourier-transform infrared (FTIR) spectroscopies. Additionally, morphological studies using scanning electron microscopy (SEM) were conducted and the photocatalytic and self-cleaning properties of the film were studied.

2. Experimental

2.1. Materials

Ammonium hexafluorotitanate (IV) ($[NH_4]_2TiF_6$, *M*w: 197.93) was purchased from Morita Chemical Industries, Japan. Boric acid (H_3BO_3), hydrochloric acid (HCl, 1.0 M) and ammonia (NH_3, 30 wt% in H_2O) were purchased from Wako Pure Chemicals, Japan. Tetrakis(*N*-methylpyridinium-4-yl)porphine, tetrakis(*p*-toluenesulfonate) (TMPyP, *M*w: 1363.61) was purchased from Tokyo Kasei, Japan. Acetic acid and aromatic carboxylic acids (ACAs, Scheme 1), including 4-aminobnzoic, 4-nitrobenzoic, phthalic, isophthalic, trimellitic, and mellitic acids, were purchased from Tokyo Kasei, Japan. All reagents used were of analytical grade and used without further purification. Deionized pure water (18.2 Ω·cm, Aquapuri 541; Young In Scientific, Korea) was obtained by reverse osmosis followed by ion exchange and filtration.

2.2. Modification of LPG optical fibers using imprinted TiO_2 films

The process of modifying the surface of the optical fiber LPG with a molecularly imprinted film is illustrated in Scheme 2. In brief, the section of fiber containing the LPG was immersed in an LPD reaction solution containing $(NH_4)_2TiF_6$ (100 mM), H_3BO_3 (500 mM), and TMPyP (1.0 mM) aqueous solutions (($(NH_4)_2TiF_6$:H_3BO_3:TMPyP = 4.5:4.5:1, *v*/*v*]. After the deposition, the TMPyP/TiO_2 film-modified LPG was kept in an oven at 60 °C (humidity 90%) for 12 h. A non-imprinted TiO_2 film-forming solution was prepared by mixing a 100 mM $(NH_4)_2TiF_6$ aqueous solution with a 500 mM H_3BO_3 aqueous solution at a ratio of 1:1. The TMPyP/TiO_2 film was also deposited onto a quartz substrate in the same manner as that used for the preparation of the LPG sensor. The composition and optical responses of the films were confirmed using a UV–vis spectrophotometer (V-570; JASCO, Japan). Fluorescence images of the TMPyP/TiO_2 film were recorded using a fluorescence microscope (Stereo Lumar V12, Carl Zeiss).

2.3. Imprinting effect and guest selectivity

Transmission spectra (TS) of the LPG were acquired by coupling the output from a tungsten-halogen lamp (HL-2000; Ocean Optics, USA) into the optical fiber and analyzing the transmitted light using a fiber-coupled CCD spectrometer (HR-2000; Ocean Optics, USA). The TMPyP/TiO_2 film was immersed into 0.01 M of HCl for 15 min to remove the TMPyP template. Additionally, the TMPyP-imprinted film (hereinafter defined as MI-film) was treated with aqueous ammonia solution (5 wt%) for 5 min in order to make the charge of the film negative before template rebinding. TMPyP template rebinding was conducted by immersing the LPG sensor into a TMPyP solution (0.1 mM

in water) for 15 min. Selectivity testing was also performed using acetic acid and ACA guest molecules (1–1000 μM in water) for 15 min. Usually, organic carboxylic acids are capable of making strong complexes with TiO_2 and thus ACAs were chosen for selectivity tests. The TS were recorded with the LPG in water and in air, before and after exposure to TMPyP and to the ACAs. For FTIR measurements, a TMPyP/TiO_2 film was prepared on a gold-coated glass plate in the same manner and measured using a Spectrum 100 FTIR spectrometer (Perkin Elmer Japan Co., Ltd.).

2.4. Photodegradation of the template

For SEM measurements and photodegradation characterization, the MI-film was deposited onto a silicon wafer (2×2 cm^2) in the same manner as that used to prepare the LPG sensor. SEM measurements were performed using a Hitachi S-5200 apparatus. For the photodegradation experiments, a TMPyP solution (10 μM, 4 mL) was placed into a plastic cell with the silicon wafer coated with an MI-film. A UV light (100 V, 6 W, λ = 352 nm, SANHAYATO, Japan) served as the UV light source. The absorption spectrum of the solution was measured at 30 min intervals.

3. Results and discussion

3.1. Evaluation of film deposition

The LPG acts to couple light from the forward propagating mode of the core of the fiber to a discrete set of co-propagating cladding modes at wavelengths governed by the phase matching condition (Eq. 1),

$$\lambda_{(x)} = (n_{core} - n_{clad(x)})\,\Lambda \quad (1)$$

where $\lambda_{(x)}$ represents the wavelength at which coupling occurs to the linear polarized

(LP_{0x}) mode, n_{core} is the effective refractive index of the mode propagating in the core of the fiber, $n_{clad(x)}$ is the effective index of the LP_{0x} cladding mode, and Λ is the period of the grating. The behaviour of the TS of LPGs of period equal to that reported here has been well described in previous articles [30–33], where it has been shown to be sensitive to changes in the optical thickness of coatings deposited onto the surface of the cladding of the optical fiber.

Figure 1 shows the evolution of the TS of the LPG when immersed into the film forming solution. As the TiO_2 film increases in optical thickness, the central wavelengths of the attenuation bands corresponding to coupling to the LP_{020}, LP_{019} and LP_{018} cladding modes (at 652 nm, 610 nm and 575 nm, respectively), undergo small blue shifts until the optical thickness of the coating is such that the mode transition region is accessed[34,35], after approximately 900 s. At the mode transition region, one of the cladding modes becomes phase matched to the waveguide formed by the coating and is no longer guided, resulting in a reorganisation of the cladding modes and a region of enhanced sensitivity to changes in coating properties, evidenced by the rapid blue shift in the attenuation bands' wavelengths. In this case, the period of the LPG has been optimised such that the phase matching turning point (PMTP) is also accessed for a coating of this optical thickness. At the PMTP, the LPG's phase matching condition is such that coupling to a higher order cladding mode, in this case LP_{021}, is achieved. The coincidence of the PMPT and the mode transition region is known to allow optimum sensitivity. As the film grows further, the LP band deepens before splitting into two [36]. The faints bands seen to the red wavelength sides of the LP_{018}, LP_{019} and LP_{020} attenuation bands during the mode transition region, and the band that forms after approximately 1200 s centred at 775 nm, are attributed to coupling to hybrid modes, which are typically observed when the

refractive index of the coating has an imaginary component, corresponding to losses due to absorption or scattering [34,36,37].

Figure 2a (Figure S1a) shows the TS of the optical fiber LPG before and after deposition of the TMPyP/TiO_2 film for 4.5 h, and after heat treatment at 60 °C for 12 h, measured in air and in water. Three LPG resonance bands with central wavelengths of ca. 692, 775, and 888 nm are newly observed after 4.5 h deposition. During LPD film deposition, the transmission decreases at 775 nm as the resonance band at the phase matching turning point is formed. The band at around 775 nm splits into two bands (known as dual resonance bands) at around 692 nm (1st band) and 888 nm (2nd band) after film deposition for 4.5 h. These changes in TS of the LPG, which are typical and usually observed at the coating of the LPG with nanothin films [31,32], indicate an increase of the optical thickness of the TMPyP/TiO_2 film. The shoulders on the blue wavelength edge of the band at 888 nm and the red wavelength edge of the band at 692 nm correspond to coupling to the hybrid modes described in Figure 1, as does the band at 775 nm. Furthermore, a blue shift of the 1st resonance band at around 690 nm and a red shift of the 2nd resonance band at around 905 nm are observed following heat treatment. This suggests that the degree of crystallinity of the TiO_2 coating increases upon heat treatment. As a result, the RI of the TMPyP/TiO_2 film is enhanced. To calibrate the RI sensitivity of the TMPyP/TiO_2 film-modified LPG sensor, aqueous solutions containing different sucrose concentrations were used (Figure S2). TMPyP is shown to be successfully incorporated into the TiO_2 matrix during the LPD process.

Upon the deposition of the non-imprinted film (hereinafter defined as NI-film), the TS of the LPG undergoes similar changes. After heat treatment, the 1st and 2nd resonance bands of the NI-film modified LPG, which were found originally at around 711 and 847

nm, are also shifted in opposite directions to 700 and 874 nm, respectively, as shown in Figure 2b (Figure S1b). The band separation of the 1st and 2nd resonance bands before and after heat treatment is much bigger in the TMPyP/TiO_2 film than in the NI-film. This larger band separation appears to be caused by the increase in the RI owing to the incorporation of TMPyP in the film [38,39].

Figure 3 compares the surface morphology of the TMPyP/TiO_2 film and of the NI-film before and after heat treatment at 60 °C for 12 h. The NI-film is deposited on the silicon substrate by forming relatively large non-uniform particles (ca. 50–100 nm) (Figure 3a). In contrast, the TMPyP/TiO_2 film is formed from uniform nanosized particles (ca. 5–10 nm) (Figure 3c), which helps in improving sensing performance by increasing the surface area and also provides precise binding sites for the template. No structural changes are seen following heat treatment at 60 °C for both films (Figures 3b and d). The insets in Figures 3b and d show photographs of the NI-film and TMPyP/TiO_2 film, respectively, created on silicon substrates. The TMPyP/TiO_2 film is more transparent than the NI-film, indicating that smaller TiO_2 particles were formed in the TMPyP/TiO_2 film.

3.2. Sensitivity and selectivity of the sensor

The LPD-based TiO_2 film can be deposited onto the surface of the optical fiber according to the reactions in Eqs. 2 and 3. The surface of TiO_2 is readily hydroxylated in aqueous solution to form two distinctive hydroxyl groups (Eq. 4). It is thought likely that TMPyP is incorporated into the TiO_2 matrix via ion-exchange reaction of hydroxyl groups of TiO_2 with *p*-toluenesulfonate (*p*-CH_3-ph-SO_3^-) counter anions of the TMPyP (Eq. 5). The pH of the surrounding aqueous solution influences the surface state of the TiO_2, with surface charges being balanced at a certain pH. The surface charge of the as-prepared

TMPyP/TiO_2 film can be controlled in accordance with the acid-base equilibria in Eqs. 6 and 7, which correspond to lower pH (HCl treatment) and higher pH (ammonia treatment), respectively. The HCl treatment of the film makes the electrostatic interaction between the TMPyP and TiO_2 matrix weak. Consequently, the TMPyP molecules can be removed from the film.

$$(NH_4)_2TiF_6 + 2H_2O \rightarrow TiO_2 + 2NH_4F + 4HF \quad (2)$$

$$H_3BO_3 + 4HF \rightarrow BF_4^- + H_3O^+ + 2H_2O \quad (3)$$

$$Ti–O–Ti + H_2O \rightarrow 2TiOH \quad (4)$$

$$4TiOH + TMPyP^{4+}(4p\text{-}CH_3\text{-}ph\text{-}SO_3^-) \rightarrow$$

$$4TiO^- + TMPyP^{4+} + 4p\text{-}CH_3\text{-}ph\text{-}SO_3H \quad (5)$$

$$TiO^- + H^+ \rightarrow TiOH \quad (6)$$

$$TiOH + OH^- \rightarrow TiO^- + H_2O \quad (7)$$

To confirm the imprinting of TMPyP, the TMPyP/TiO_2 film was immersed in HCl (0.01 M) for 15 min. As a result, the reduction in the RI of the coating caused wavelength shifts of the 1st and 2nd resonance bands from 690 and 905 nm to 738 and 815 nm, respectively, as shown in Figure 4a (Figure S3a). This indicates that the TMPyP template molecules are completely removed from the TMPyP/TiO_2 film. Subsequently, template rebinding into the matrix with prior treatment of the LPG in 5 wt% ammonia solution was performed. Significant wavelength shifts of the LPG resonance bands were observed upon rebinding the template into the matrix following treatment with ammonia, indicating that the negatively charged surface of the MI-film, which is described in Eq. 7, promotes the adsorption of TMPyP. Therefore, the same ammonia treatment of the MI-film for 5 min was applied to all guest binding tests.

The responses of the MI-film-modified LPG sensor to different concentrations of TMPyP are also shown in Figure 4a. The wavelength shifts of the resonance bands become more pronounced as the concentration of TMPyP increases from 1.0 to 100 μM. The 2nd resonance band shows red shifts of 31, 72, 76, and 87 nm for TMPyP concentrations of 1.0, 10, 50, and 100 μM, respectively. Changes in the TS of the dried MI-film after TMPyP adsorption are also observed (Figure S3b). In contrast, the 1st resonance band shows a blue shift of 47 nm upon 100 μM TMPyP rebinding. These wavelength shifts are significantly larger than those obtained using the NI-film (Figure 4b). It is well-known that TMPyP is a two-photon dye, showing a red color upon UV excitation. As evident in Figure S4, the fluorescence of TMPyP disappears completely upon exposure of the TMPyP/TiO_2 film to HCl (0.01 M), and is restored after TMPyP (100 μM) rebinding, indicating that the fabrication of the MI-film was successful and molecularly imprinted sites for TMPyP rebinding were created in the film.

Figure 4c shows the calibration curves corresponding to wavelength shifts of the 1st and 2nd resonance bands of the TS recorded in water, and of the 2nd resonance band of the TS recorded in air, for different concentrations of TMPyP. The LPG shows significant wavelength shifts of the resonance bands after treatment with 10 μM of TMPyP. For concentrations above 10 μM, the LPG sensor signal reaches saturation and it can be seen that the MI-film-modified LPG sensor is highly sensitive to the template. Consequently, the dissociation constant (K_d), which was obtained using the wavelength shifts of the 2nd resonance band recorded in water, is estimated to be $1.95 \pm 0.20 \times 10^{-6}$ M. This value is very close to the reciprocal (1.67×10^{-6} M) of the binding constant (K_a) that has been obtained from the Benesi–Hildebrand plot (see the Electronic Supporting Material). Similarly, K_a and K_d values can be also obtained using the wavelength shifts of the 1st

resonance band recorded in water, which are summarized in Table S1.

The MI-film-modified LPG sensor exhibited similar sensitivity to TMPyP molecules after 5 days of use. However, a remarkable decrease in the sensitivity of the MI-film was observed after 10 days (Figure S5). Plausibly, this is because the imprinted cavities are polluted as the film was left under ordinary room conditions.

The selectivity of the MI-film and imprinting effect were tested with TMPyP (100 μM), acetic acid (1000 μM), and the ACAs (1000 μM) in water (Figures 5a and S6a) and in air (Figure S7). Upon exposure to TMPyP, the LPG sensor made with the MI-film shows wavelength shifts for the 1st and 2nd resonance bands that are 4.6 and 30.5 times larger than those of the sensor made with the NI-film, respectively. The MI-film led to substantial wavelength shifts of the two resonance bands in the range of 19−31 nm for MA and TA, significantly larger than those observed in response to the other chemicals. The wavelength shifts of the resonance bands of the MI-film-modified LPG sensor when exposed to BA, i-Pa, NH_2-BA, PA, and NO_2-BA are much smaller than those observed when exposed to the template. To confirm the efficiency of the molecular imprinting, the response of the NI-film-modified LPG sensor to TMPyP and the ACAs was examined (Figure 5b).

Figure 6 compares the wavelength shifts of the 1st and 2nd resonance bands upon exposure to the template and guest molecules for the MI- and NI-films. The NI-film shows small responses to all the tested compounds in a wavelength shift range of 2−7 nm. Interestingly, MA and TA in both MI- and NI-films show relatively large binding compared to the template. This response might be attributed the intermolecular hydrogen bonding in cases of MA and TA, because they have six and three carboxyl groups in a molecule, respectively. Among them, some carboxylic acids are used for forming intra-

and intermolecular hydrogen bonds, for which water molecules are excluded from the film. Therefore, we can conclude that structural analogues or other molecules have no effect on the identification of the target molecule.

The removal and rebinding of the TMPyP template are confirmed in the FTIR measurement results (Figure 7). Relatively large vibration bands in the range 500−700 cm^{-1} originate from the Ti−O−Ti bond, which are observed in all samples. The peaks at 1641 and 1186 cm^{-1} are due to the stretching vibrations of the C=N group in the pyridinium and pyrrole rings of TMPyP in the hybrid. Additionally, the presence of TMPyP can be confirmed from the peak for the out-of-plane bending vibration for the C–H bonds of the *p*-substituted pyridines near 815 cm^{-1}. These peaks disappear upon exposure of the film to HCl (0.01 M), and are restored after TMPyP (0.1 mM) rebinding. Interestingly, a broad band is observed at around 1665 cm^{-1} after template removal, which may be assigned to the O−H vibrations due to the presence of adsorbed water in the film. This band disappears after template rebinding and the peak at 1641 cm^{-1} is restored, suggesting that the water was removed from the film, owing to the rebinding of TMPyP.

3.3. Photocatalytic and self-cleaning performances

To confirm the photocatalytic performance of the MI-film, the UV–vis absorption spectrum of the MI-film deposited on a quartz plate was investigated before and after heat treatment and upon TMPyP removal and rebinding, as shown in Figure 8a. The absorbance in the 200–250 nm region increases with increasing temperature of heat treatment from room temperature to 60 °C and 90 °C, most plausibly due to an increase in the crystallinity of the TiO_2 film. All spectra of the TMPyP/TiO_2 film exhibit a typical strong Soret band for the TMPyP molecule in the 400–450 nm region, along with four

weak Q bands in the 500–700 nm region. It can be seen that complete removal of the TMPyP is achieved after 15 min treatment with HCl. Interestingly, TMPyP rebinding after ammonia treatment completely recovers the intensity of the TMPyP Soret band to that measured before template removal.

Figure 8b shows the decrease in the dye concentration upon irradiation with UV light (λ = 352 nm). Compared with the MI-film without heat treatment, both heat-treated MI-films exhibit substantial enhancement of photocatalytic activity for template irradiation. TMPyP is completely decomposed in the films with heat treatment at 60 and 90 °C under UV irradiation for 300 min. According to these results, it is clear that the MI-films prepared with heat treatment have better crystallinity, suggesting that a synergy effect of molecular imprinting and heat treatment promotes the photocatalytic activity of the MI-films.

The 1st and 2nd resonance bands of the MI-film-modified LPG exhibited shifts in opposite directions of 46 and 80 nm under UV irradiation, and of 45 and 76 nm under indoor visible light (Figure 9a). Figure 9b compares the dynamic intensity changes of the MI-film-modified LPG sensor measured at 800 nm. The rate of adsorption of TMPyP is faster in the first 10 min under UV irradiation than under indoor visible light. Interestingly, photodegradation of TMPyP under UV irradiation occurs after its saturated adsorption. The increased adsorption of TMPyP under UV irradiation can be explained by the following two factors: First, the increased negative charge density of binding sites due to UV irradiation and the enhanced electrostatic interactions between the template molecule and the activated TiO_2 matrix. Second, the degradation of impurities adhering by physical adsorption to the MI-film. Plausibly, these factors will provide further active sites for template rebinding and photodegradation.

For the first time, to the best of our knowledge, the self-cleaning properties of molecularly imprinted TiO_2 nanothin films were combined with an optical fiber sensor, which enabled real-time monitoring of the decomposition process. This could be particularly advantageous in an application such as air filters, where TiO_2 could be coated onto the fibers of the filter and the sensor could monitor, and allow control of, the level of contamination and hence enhance the lifetime of the filter. The flexibility of the molecular imprinting technique would allow enhancement of the binding capacity toward particular air-borne chemical and bio-contaminates [17–21].

One of the key limitations of the use of TiO_2 for molecular imprinting is the limited availability of the functional groups that can provide stronger affinity towards particular analytes. This can be improved by combining molecularly imprinted inorganic matrices with organic moieties that can increase number of functional groups and hence improve selectivity.

4. Conclusions

In this study, a novel molecular imprinting technique based on TiO_2 nanothin films coupled with an optical fiber LPG was demonstrated. The cationic porphyrin compound TMPyP, which has four *N*-methylpyridinium moieties along with four *p*-toluenesulfonate counter anions, was used for complexation with the TiO_2 matrix. There are a lot of cationic compounds, including organic dyes and metal ion complexes, in the environment. From this perspective, the TMPyP used in this study would provide the possibility, as a preliminary study, for the molecular imprinting of positively charged chemicals and macrocyclic biological molecules. Imprinted and non-imprinted TiO_2 nanothin films were prepared via LPD of a mixture of $(NH_4)_2TiF_6$ and H_3BO_3 with and without the template,

respectively. The TMPyP-imprinted TiO_2 film showed higher sensitivity and selectivity towards the template molecule than to ACAs as guest molecules, providing a large wavelength shift of several tens of nanometers. In addition, the adsorption of TMPyP could be further improved under UV irradiation, which may be attributed to the increased negative charge density of binding sites due to UV irradiation; however, photodegradation of TMPyP occurs after its adsorption was saturated. Furthermore, impurities bound to the imprinted film could be completely decomposed through self-cleaning under UV irradiation by exploiting the photocatalytic properties of TiO_2. We believe that the current approach provides a useful methodology for new creation of sensing devices coupled with molecularly imprinted materials. In particular, the self-cleaning ability of TiO_2 might be helpful in preventing the contamination of binding sites, resulting in long-term stability and high efficiency of the device.

Acknowledgments

The authors would like to thank Mr. Shichiro Yoshinobu for his technical support of photocatalytic evaluation of TMPyP. The analysis of the samples was partly conducted at the Instrumentation Center, the University of Kitakyushu.

References

1. Eersels, K.; Lieberzeit, P.; Wagner, P. Review on Synthetic Receptors for Bioparticle Detection Created by Surface-Imprinting Techniques from Principles to Applications. *ACS Sens*. **2016**, *1*, 1171–1187.
2. Yang, D. H.; Takahara, N.; Lee, S. W.; Kunitake, T. Fabrication of glucose-sensitive TiO_2 ultrathin films by molecular imprinting and selective detection of monosaccharides. *Sensor. Actuat. B-Chem.* **2008,** *130*, 379–385.
3. Han, Q.; Shen, X.; Zhu, W.; Zhu, C.; Zhou, X.; Jiang, H. Magnetic sensing film based on Fe_3O_4@Au-GSH molecularly imprinted polymers for the electrochemical detection of estradiol. *Biosens. Bioelectron.* **2016**, *79*, 180–186.
4. Xue, C.; Han, Q.; Wang, Y.; Wu, J.; Wen, T.; Wang, R.; Hong, J.; Zhou, X.; Jiang, H. Amperometric detection of dopamine in human serum by electrochemical sensor based on gold nanoparticles doped molecularly imprinted polymers. *Biosens. Bioelectron.* **2013**, *49*, 199–203.
5. Li, Y.; Ding, M.; Wang, S.; Wang, R.; Wu, X.; Wen, T.; Yuan, L.; Dai, P.; Lin, Y.; Zhou, X. Preparation of Imprinted Polymers at Surface of Magnetic Nanoparticles for the Selective Extraction of Tadalafil from Medicines. *ACS Appl. Mater. Interfaces* **2011**, *3,* 3308–3315.
6. Yoshikawa, M.; Tharpa, K.; Dima, S. O. Molecularly Imprinted Membranes: Past, Present, and Future. *Chem. Rev.* **2016**, *116*, 11500–11528.
7. Luo, J.; Gao, Y. H.; Tan, K.; Wei, W.; Liu, X. Y. Preparation of a Magnetic Molecularly Imprinted Graphene Composite Highly Adsorbent for 4-Nitrophenol in Aqueous Medium. *ACS Sustainable Chem. Eng*. **2016**, *4*, 3316−3326.
8. Liu, Y. X.; Cao, B.; Jia, Peng.; An, J. H.; Luo, C.; Ma, L. J.; Chang, J.; Pan, K. Layer-

by-Layer Surface Molecular Imprinting on Polyacrylonitrile Nanofiber Mats. *J. Phys. Chem. A* **2015**, *119*, 6661–6667.

9. Wang, C. H.; Li, C. Y.; Wei, L. F.; Wang, C. F. Electrochemical sensor for acetaminophen based on an imprinted TiO_2 thin film prepared by liquid phase deposition. *Microchim. Acta* **2007**, *158*, 307–313.
10. Mizutani, N.; Yang, D. H.; Selyanchyn, R.; Korposh, S.; Lee, S. W.; Remarkable enantioselectivity of molecularly imprinted TiO_2 nano-thin films. *Anal. Chim. Acta* **2011**, *694*, 142–150.
11. Wybranska, K.; Niemiec, W.; Szczubiazka, K.; Nowakowska, M.; Morishima, Y. Adenine Molecularly Imprinted Polymer-Coated Submicrometer Silica Gel Particles. *Chem. Mater*. **2010**, *22*, 5392–5399.
12. Murase, N.; Taniguchi, S. I.; Takano, E.; Kitayama, Y.; Takeuchi, T. A molecularly imprinted nanocavity-based fluorescence polarization assay plat form for cortisol sensing. *J. Mater. Chem*. **2016**, *4*, 1770–1777.
13. Lee, S. W.; Ichinose, I.; Kunitake, T. Molecular Imprinting of Azobenzene Carboxylic Acid on a TiO_2 Ultrathin Film by the Surface Sol-Gel Process. *Langmuir* **1998**, *14*, 2857–2863.
14. Lee, S. W.; Ichinose, I.; Kunitake, T. Molecular imprinting of protected amino acids in ultrathin multilayers of TiO_2 gel. *Chem. Lett.* **1998**, *27*, 1193–1194.
15. Araki, K.; Yang, D.-H.; Wang, T.; Selyanchyn, R.; Lee, S.-W.; Kunitake, T. Self-assembly and imprinting of macrocyclic molecules in layer-by-layered TiO_2 ultrathin films. *Anal. Chim. Acta* **2013**, *779*, 72–81.
16. Zhang, C.; Si, S.; Yang, Z. A highly selective photoelectrochemical biosensor for uric acid basedon core–shell Fe_3O_4@C nanoparticle and molecularly imprinted TiO_2,

Biosens. Bioelectron. **2015**, *65*, 115–120.

17. Zhang, Y. N.; Dai, W.; Wen, Y.; Zhao, G. Efficient enantioselective degradation of the inactive (S)-herbicide dichlorprop on chiral molecular-imprinted TiO_2. *Appl. Cat. B: Environmental* **2017**, *212*, 185–192.
18. Escobar, C. C.; Ruiz, Y. P. M.; Santos, J. H. Z.; Ye, L. Molecularly imprinted TiO_2 photocatalysts for degradation of diclofenac in water. *Colloids Surf. A* **2018**, *538*, 729–738.
19. Escobar, C. C.; Lansarin, M. A.; Santos, J. H. Z. Synthesis of molecularly imprinted photocatalysts containing low TiO_2 loading: Evaluation for the degradation of pharmaceuticals. *J. Hazard. Mater*. **2016**, *306*, 359–366.
20. Shen, X.; Zhu, L.; Li, J.; Tang, H. Synthesis of molecular imprinted polymer coated photocatalysts with high selectivity. *Chem. Commun*. **2007**, 1163–1165.
21. Shen, X.; Zhu, L.; Liu, G.; Yu, H.; Tang, H. Enhanced Photocatalytic Degradation and Selective Removal of Nitrophenols by Using Surface Molecular Imprinted Titania. *Environ. Sci. Technol.* **2008**, *42*, 5, 1687–1692.
22. Tatemichi, M.; Sakamoto, M.; Mizuhara, M.; Deki, S.; Takeuchi, T. Protein-Templated Organic/Inorganic Hybrid Materials Prepared by Liquid-Phase Deposition. *J. Am. Chem. Soc*. **2007**, *129*, 10906–10910.
23. Feng, L.; Liu, Y. J.; Hu, J. M. Molecularly Imprinted TiO_2 Thin Film by Liquid Phase Deposition for the Determination of *L*-Glutamic Acid. *Langmuir* **2004**, *20*, 1786–1790.
24. Schneider, J.; Matsuoka, M.; Takeuchi, M.; Zhang, J. L.; Horiuchi, Y.; Anpo, M.; Bahnemann, D. W. Understanding TiO_2 Photocatalysis: Mechanisms and Materials. *Chem. Rev*. **2014**, *114*, 9919–9986.

25. Chen, X. B.; Liu, L.; Yu, P. Y.; Mao, S. S. Increasing Solar Absorption for Photocatalysis with Black Hydrogenated Titanium Dioxide Nanocrystals. *Science* **2011**, *331*, 746–750.

26. Afzal, S.; Daoud, W. A.; Langford, S. J. Photostable Self-Cleaning Cotton by a Copper(II) Porphyrin/TiO_2 Visible-Light Photocatalytic System. *ACS Appl. Mater. Interfaces* **2013**, *5*, 4753−4759.

27. Xi, B.; Verma, L. K.; Li, J.; Bhatia, C. S.; Danner, A. J.; Yang, H.; Zeng, H. C. TiO_2 Thin Films Prepared via Adsorptive Self-Assembly for Self-Cleaning Applications. *ACS Appl. Mater. Interfaces* **2012**, *4*, 1093–1102.

28. Antony, R. P.; Mathews, T.; Dash, S.; Tyagi, A. K. Kinetics and Physicochemical Process of Photoinduced Hydrophobic ↔ Superhydrophilic Switching of Pristine and N-doped TiO_2 Nanotube Arrays. *J. Phys. Chem. C* **2013**, *117*, 6851−6860.

29. James, S. W.; Tatam, R. P. Optical fiber long-period grating sensors: Characteristics and application. *Meas. Sci. Technol*. **2003**, *14*, 49−61.

30. Korposh, S.; Lee, S. W.; James, S. W.; Tatam, R. P. Refractive index sensitivity of fiber-optic long period gratings coated with SiO_2 nanoparticle mesoporous thin films. *Meas. Sci. Technol*. **2011**, *22*.

31. Korposh, S.; Wang, T.; James, S. W.; Tatam, R. P.; Lee, S. W. Pronounced aromatic carboxylic acid detection using a layer-by-layer mesoporous coating on optical fiber long period grating. *Sensor. Actuat. B-Chem.* **2012,** *173*, 300−309.

32. Wang, T.; Korposh, S.; James, S. W.; Tatam, R. P.; Lee, S. W. Optical fiber long period grating sensor with a polyelectrolyte alternate thin film for gas sensing of amine odors. *Sensor. Actuat. B-Chem.* **2013**, *185,* 117−124.

33. Korposh, S.; Chianella, I.; Guerreiro, A.; Caygill, S.; Piletsky, S.; James, S. W.; Tatam,

R. P. Selective vancomycin detection using optical fiber long period gratings functionalised with molecularly imprinted polymer nanoparticles. *Analyst* **2014**, *139*, 2229−2236.

34. Del Villar, I.; Matias, I. R.; Arregui, F. J. Influence on cladding mode distribution of overlay deposition on long-period fiber gratings. *J. Opt. Soc. Am. A* **2006**, *23*, 651–658.
35. Cusano, A.; Iadicicco, A.; Pilla, P.; Contessa, L.; Campopiano, S.; Cutolo, A.; Giordano, M. Cladding mode reorganization in high-refractive-index-coated long-period gratings: effects on the refractive-index sensitivity. *Opt. Lett.* **2005**, *30*, 2536–2538.
36. James, S. W.; Cheung, C. S.; Tatam, R. P. Experimental observations on the response of 1st and 2nd order fibre optic long period grating coupling bands to the deposition of nanostructured coatings. *Opt. Express* **2007**, *15*, 13096–13107.
37. Cheung, C. S.; Topliss, S. M.; James, S. W.; Tatam, R. P. Response of fiber-optic long-period gratings operating near the phase-matching turning point to the deposition of nanostructured coatings. *J. Opt. Soc. Am. B* **2008**, *25*, 897–902.
38. Gupta, B. D.; Shrivastav, A. M.; Usha, S. P. Surface plasmon resonance-based fiber optic sensors utilizing molecular imprinting. *Sensors* **2016**, *16*, 1381.
39. Yamada, Y.; Nakamura, T.; Yano, K. Optical Response of Mesoporous Synthetic Opals to the Adsorption of Chemical Species. *Langmuir*. **2008**, *24*, 2779–2784.

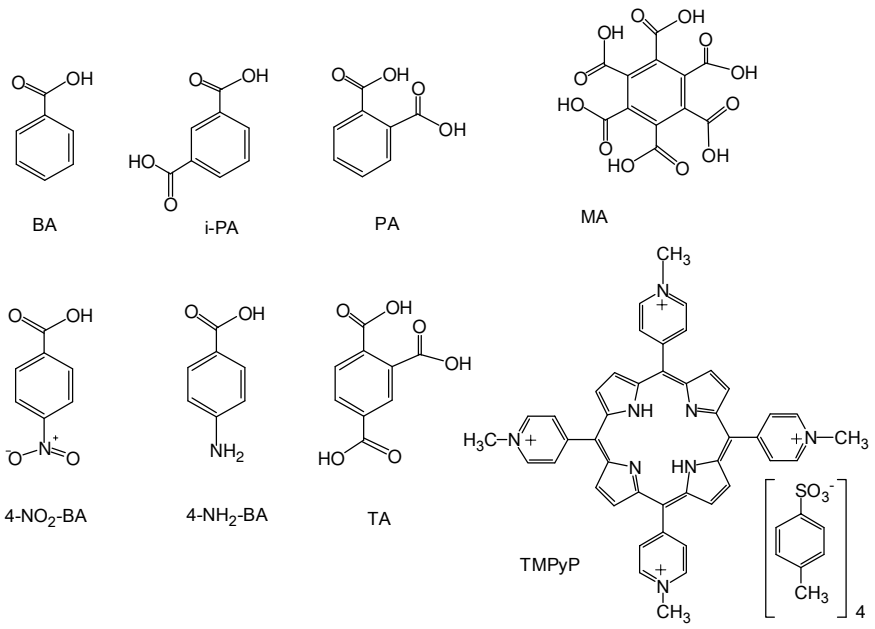

Scheme 1. Chemical structures and abbreviations of the compounds used for molecular imprinting and photodegradation experiments.

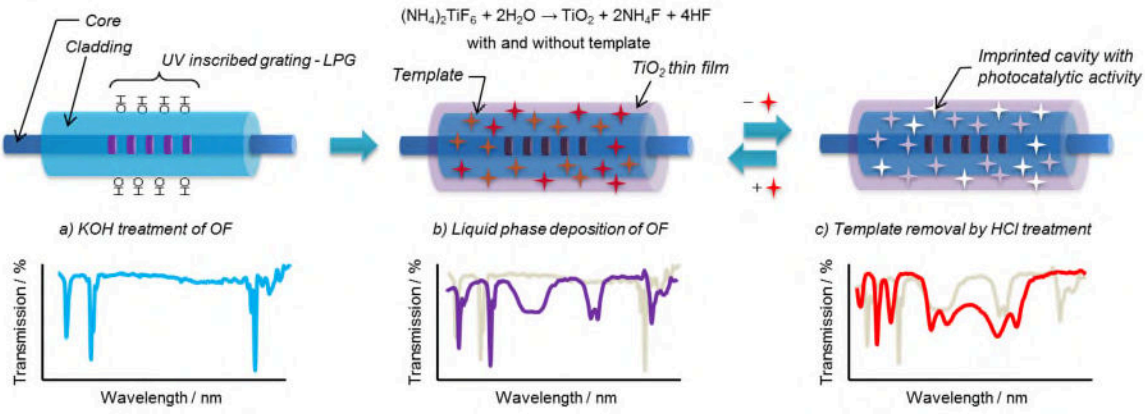

Scheme 2. Schematic illustration of the process of modifying the surface of the optical fiber LPG with a molecularly imprinted film. (a) KOH treatment to endow the surface with OH negatively charged functional groups and the corresponding LPG transmission spectrum, (b) immersion of the LPG into the film forming solution for LPD and the corresponding LPG transmission spectrum, and (c) removal of the template TMPyP using 0.01M HCl and the corresponding LPG transmission spectrum.

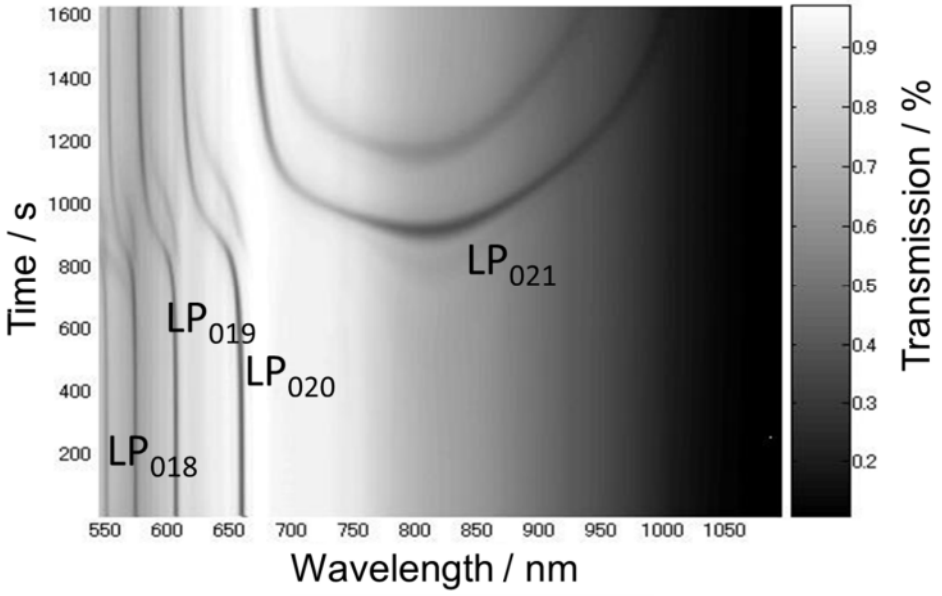

Figure 1. Evolution of the LPG's transmission spectra when immersed in a TiO_2 NI-film forming solution for 6 h. The grey scale represents the measured transmission, with white corresponding to 100% and black to 0%. The labels indicate the center wavelengths of the resonance bands and the corresponding LP modes to which fundamental mode is coupled: LP_{018} coupling to 18th LP mode at 560 nm; LP_{019} coupling to 19th LP mode at 600 nm; LP_{020} coupling to 20th LP mode at 660 nm; dual LP_{021} coupling to 21th LP mode centered at 830 nm.

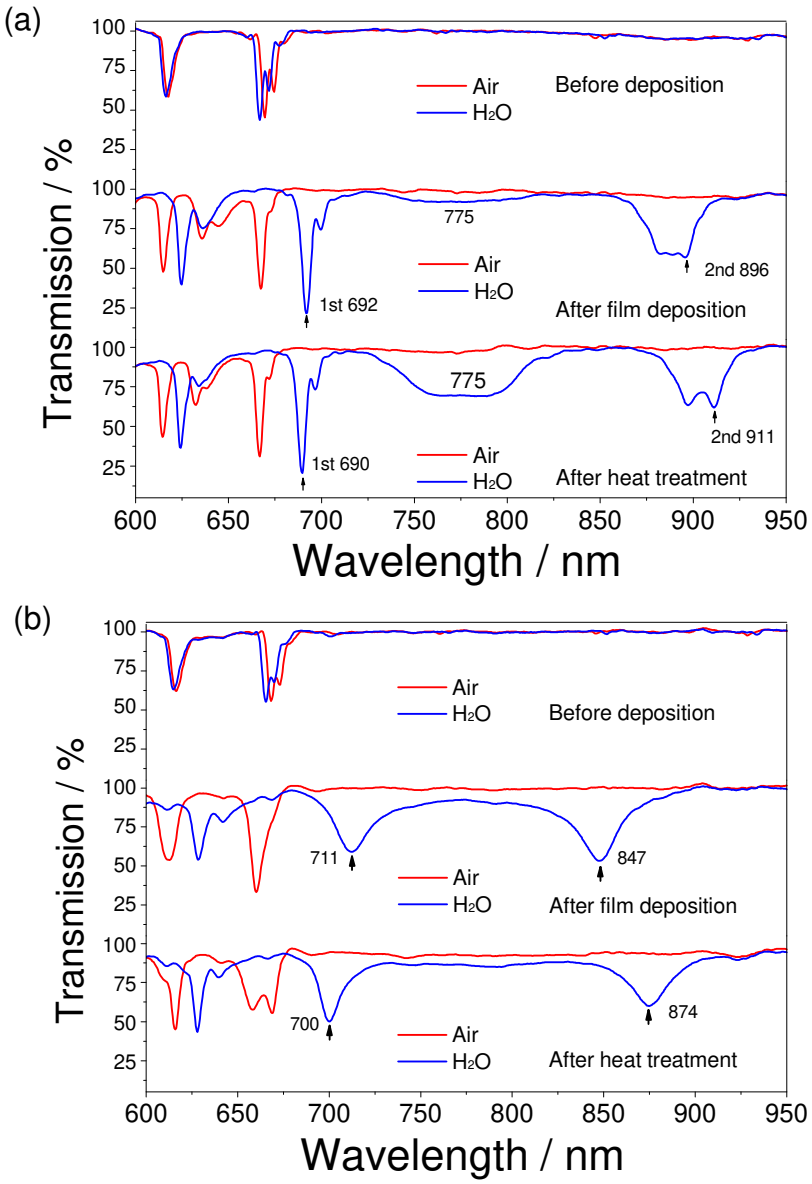

Figure 2. Transmission spectra of the LPG following deposition of the (a) TMPyP/TiO_2 film and (b) NI-film for 4.5 h and subsequently after heat-treatment at 60 °C (humidity 90 %) for 12 h, measured in water (blue line) and in air (red line), respectively. The arrows indicate the positions of the resonance bands.

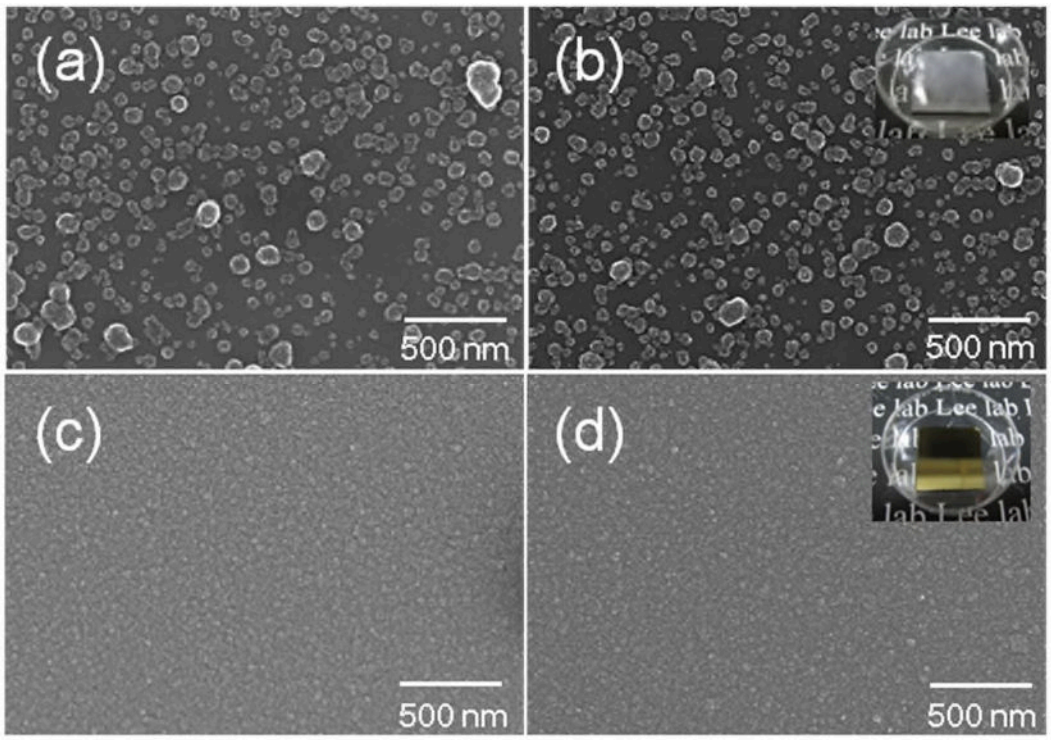

Figure 3. Comparison of the SEM images of the films deposited on silicon wafers. (a) NI-film after 4.5 h deposition and (b) after 12 h heat treatment at 60 °C. (c) TMPyP/TiO_2 film after 4.5 h deposition and (d) after 12 h heat treatment at 60 °C. The insets in (b) and (d) show photographs of the NI-film and TMPyP/TiO_2 film prepared on the silicon substrate, respectively.

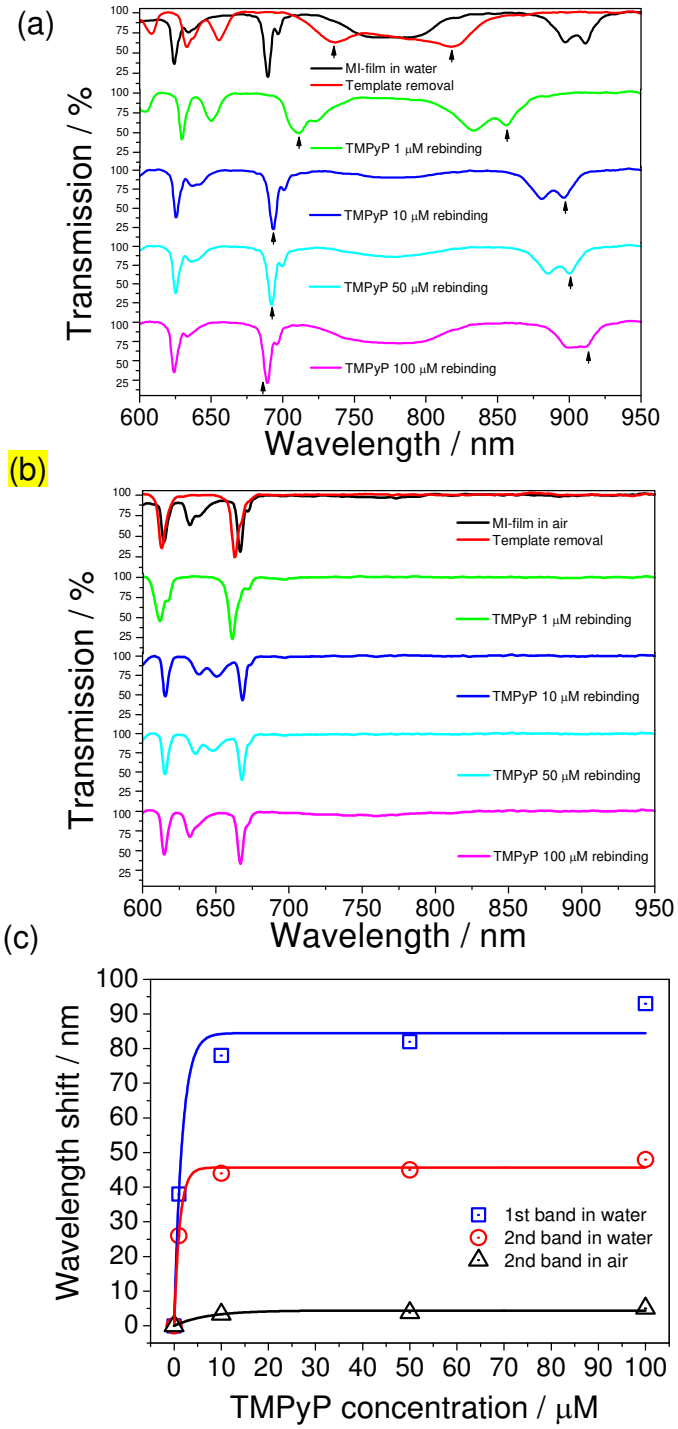

Figure 4. Transmission spectra of the MI-film-modified LPG upon rebinding with different concentrations of TMPyP in (a) water and (b) air. (c) Calibration curves plotted the from wavelength shifts of the 1st and 2nd resonance bands in water, and the 2nd resonance band in air. The arrows indicate the positions of the resonance bands.

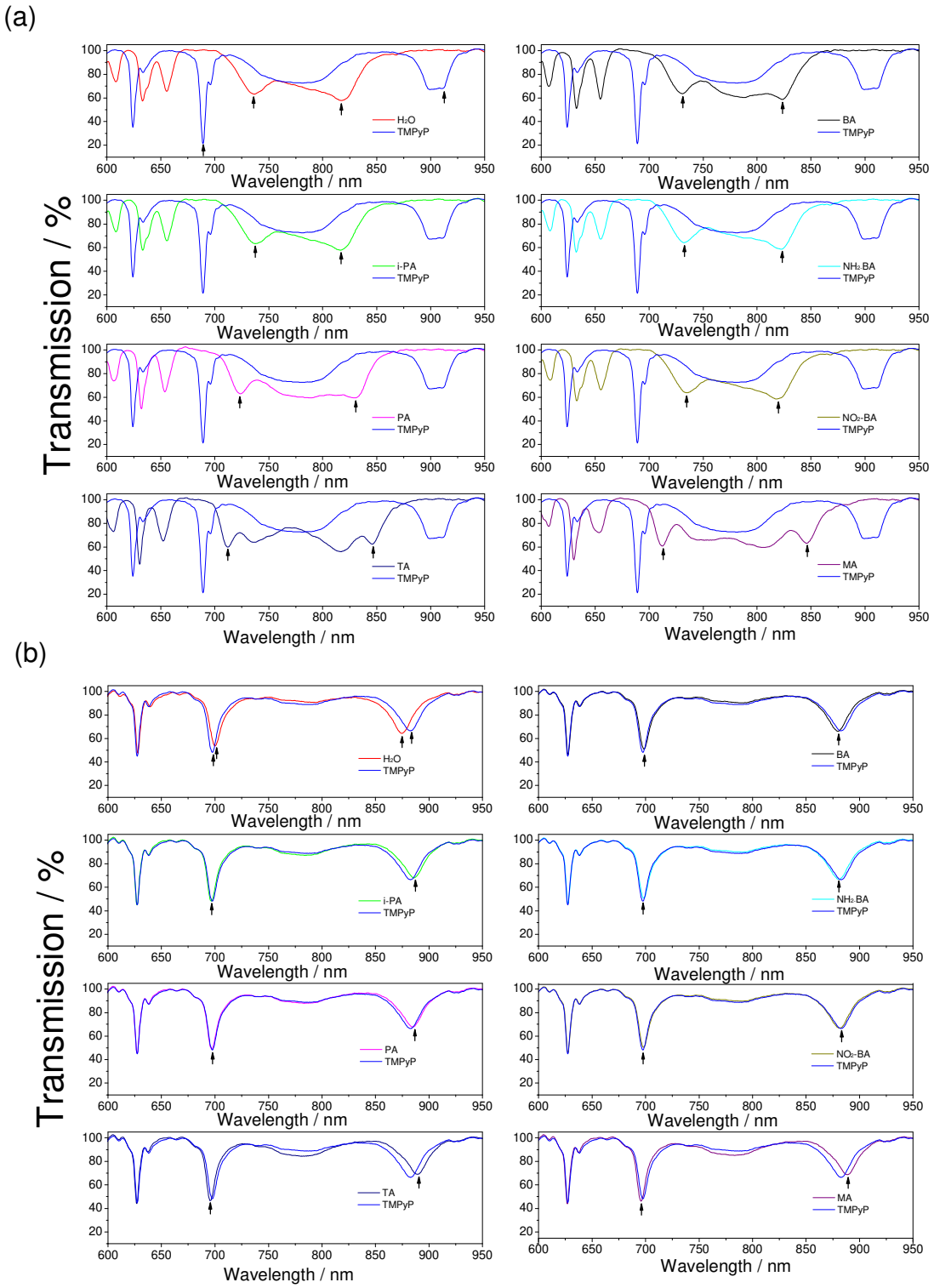

Figure 5. Changes in the transmission spectra of the (a) MI- and (b) NI-films due to exposure to different ACAs at 1.0 mM and to TMPyP at 100 uM in water. The arrows indicate the positions of the resonance bands.

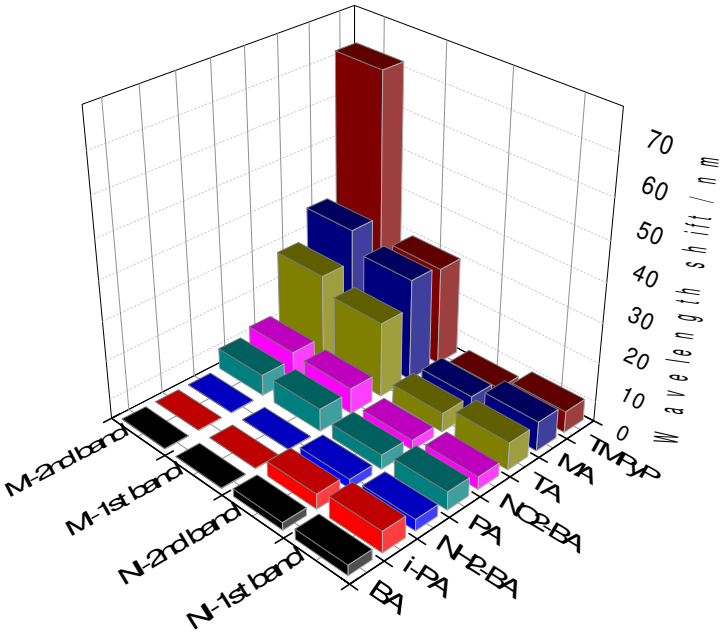

Figure 6. Comparison of the wavelength shifts upon exposure to the template and guest molecules for the MI- and NI-films.

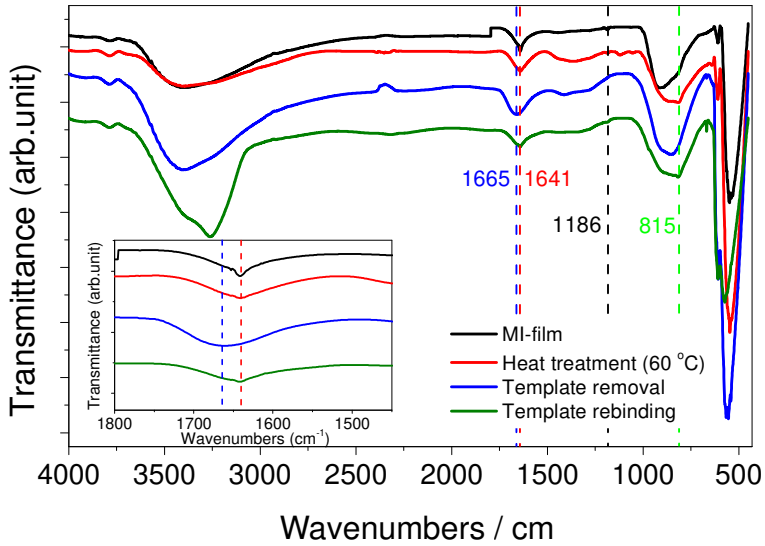

Figure 7. Comparison of FTIR spectra of the MI-film prepared on a gold-coated glass substrate for 4.5 h: (a) as deposited, (b) after heat treatment at 60 °C for 12 h, (c) after TMPyP removal in HCl (0.01 mM), and (d) after TMPyP rebinding in 0.1 mM solution.

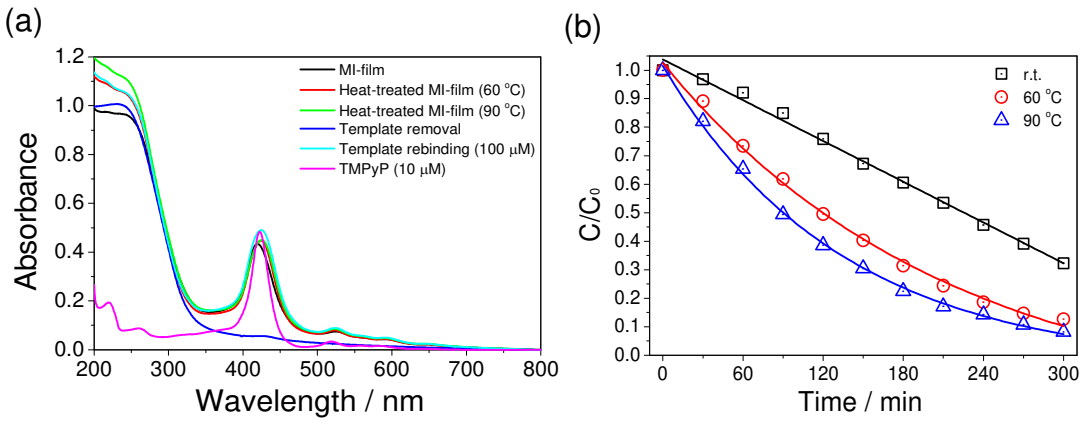

Figure 8. (a) UV–vis absorption spectra of the MI-film before and after heat treatment at 60 and 90 °C and upon TMPyP removal and rebinding in a 100 μM solution. The pink line shows the UV–vis spectrum of a TMPyP solution (10 μM). (b) The photodegradation of TMPyP on the MI-films, which are prepared without heat treatment (black line), with heat treatment at 60 °C (red line), and with heat treatment at 90 °C (blue line), under UV irradiation assessed from the absorbance at 422 nm.

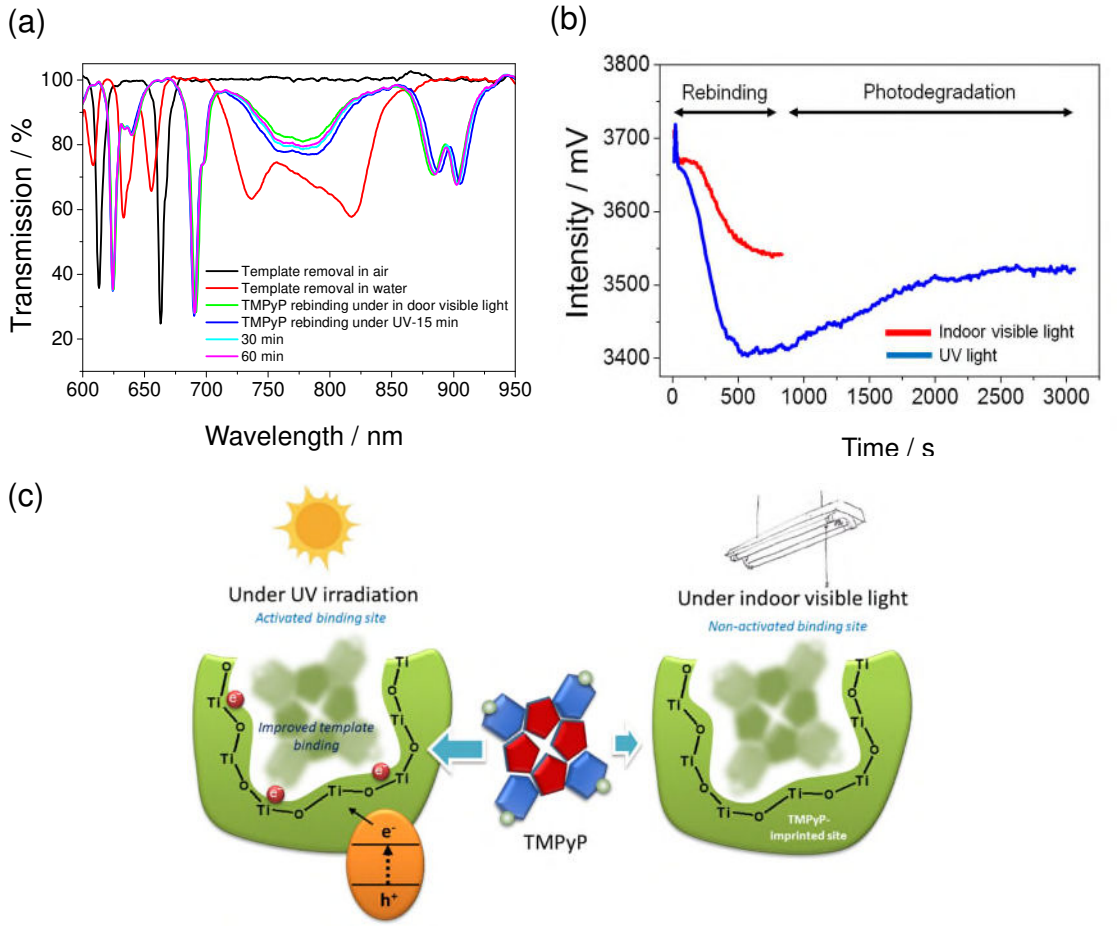

Figure 9. (a) TS of the MI-film-modified LPG sensor prepared to explore its photocatalytic activity and (b) dynamic intensity changes of the MI-film-modified LPG sensor due to TMPyP rebinding measured at 800 nm under indoor visible light and under UV irradiation. (c) Schematic illustration of improved guest binding in a molecularly imprinted photocatalytic binding site.

2020-11-17

Long-period grating fiber-optic sensors exploiting molecularly imprinted TiO2 nanothin films with photocatalytic self-cleaning ability

Wang, Tao

Springer

Wang T, Korposh S, James S, Lee SW. (2020) Long-period grating fiber-optic sensors exploiting molecularly imprinted TiO2 nanothin films with photocatalytic self-cleaning ability. Microchimica Acta, Volume 187, Issue 12, December 2020, Article number 663
https://doi.org/10.1007/s00604-020-04603-1